

A New Templated Ordered Structure with Combined Micro- and Mesopores and Internal Silica Nanocapsules

P. Van Der Voort,^{*,†} P. I. Ravikovitch,[‡] K. P. De Jong,[§] M. Benjelloun,[†] E. Van Bavel,[†]
A. H. Janssen,[§] A. V. Neimark,[‡] B. M. Weckhuysen,[§] and E. F. Vansant[†]

University of Antwerp (UIA), Department of Chemistry, Universiteitsplein 1, B-2610 Wilrijk, Belgium, Center for Modeling and Characterization of Nanoporous Materials, TRI/Princeton, P.O. Box 625, Princeton, New Jersey 08542, and University of Utrecht, Department of Inorganic Chemistry and Catalysis, Debye Institute, Sorbonnelaan 16, 3508 TB Utrecht, The Netherlands

Received: February 14, 2002

The increasing awareness of the need to create green and sustainable production processes in all fields of chemistry has stimulated materials scientists to search for innovative catalytic supports. These new catalytic supports should allow the heterogenization of most catalytic processes, increasing the efficiency and selectivity of the synthesis and reducing waste and byproducts. Following the development of several micellar templated structures, such as M41S¹, FSM-16,^{2,3} HMS,^{4,5} MSU-x,⁶ and SBA-x,^{7,8} it is a crucial next step to create support materials, consisting of a composite matrix with combined micro- and mesoporosities and a sufficient stability to withstand most industrial treatments. We describe in this paper the very first development of a hexagonal material with large pore diameters and thick walls (4 nm), containing internal microporous silica nanocapsules. These plugged hexagonal templated silicas (PHTS) have two types of micropores (originating from the walls and the nanocapsules respectively) and a tunable amount of both open and encapsulated mesopores. The micropore volumes have a high value (up to 0.3 cm³/g) and the total pore volume exceeds 1 cm³/g. The obtained materials are much more stable than the conventional micellar templated structures known so far, and can easily withstand severe hydrothermal treatments and mechanical pressures.

Introduction

Researchers of Mobil published in 1992 a breakthrough report on the synthesis of ordered mesoporous silica materials.¹ These materials were obtained by polymerizing a silica source around an organic liquid crystal template of quaternary ammonium surfactants. The publication of these results has stimulated a large and worldwide effort to synthesize new types of ordered mesoporous materials.^{2,4–11}

Due to their controlled pore size and a very narrow pore size distribution, the ordered mesoporous materials have significant potential as catalytic supports in fine chemistry, pharmaceutical industry, as well as for the production of special polymer materials.^{12–14} Heterogenizing the synthetic procedures in these fields of chemistry forms an important tool in achieving the goals of green, sustainable production processes and end-of-pipe waste reduction.¹³ Unfortunately, the actual use of the materials has been severely hampered by their poor stability. Especially the hydrothermal and mechanical stability of all these materials is below the practical level for industrial application. Therefore, there is a strong need for hydrothermally and mechanically stable structures. Moreover, materials with combined micro- and mesoporosity will offer significant supplementary advantages, such as an improved diffusion rate for transport in catalytic processes (faster reactions); better hydrothermal stability;¹⁵ multifunctionality to process a large variety of feedstocks; capabilities of encapsulated waste in the mi-

cro-pores; controlled leaching rates for a constant and gradual release of an active component, etc.

The hexagonal SBA-15 structure, prepared by triblock surfactants, developed by Stucky et al.^{7,8} is a material that has the benefits of combined micro- and mesoporosity and relatively thick silica walls. Actually, a broad range of materials was developed in Stucky's group by the use of commercially available nonionic alkyl poly(alkyleneoxide) triblock copolymers (EO_xPO_yEO_x, with EO = poly(ethylene oxide) and PO = poly(propylene oxide)) in acidic media. The hexagonal SBA-15 is the most known. SBA-15 typically has a micropore volume around 0.1 cm³/g. The micropores are created by the penetration of the hydrophobic EO chain in the silica walls, as will be discussed in more detail later.

Inagaki¹⁰ has recently further improved the synthesis of SBA-15, in order to optimize the ratio of micro- to mesopores. This adapted procedure yields materials with an increased micropore volume (0.2 cm³/g) at the expense, however, of the total pore volume and surface area (typical: 450 m²/g).

Here we describe the fast and easy synthesis of stable composite materials, with combined micro- and mesoporosity and large pore volumes. The high micropore volume and high stability of these PHTS materials is governed by internal silica nanocapsules.

Experimental Section

Materials were prepared by dissolving Pluronic P123 (non-ionic triblock copolymer, P123, EO₂₀PO₇₀EO₂₀) and TEOS (Si(OC₂H₅)₄) in various ratios (cf Table 1) in a 2 M HCl solution.

* Corresponding author. E-mail: pascal.vandervoort@ua.ac.be.

[†] University of Antwerp (UIA).

[‡] TRI/Princeton.

[§] University of Utrecht.

TABLE 1: Structural Characteristics of Selected PHTS Samples^a

sample	TEOS/P123	ageing T (K)	a_0^b (nm)	V_{tot}^c (cm ³)	S_{BET} (m ² /g)	V_{mi}^d (cm ³ /g)	V_{me}^e (cm ³ /g)	D_{pore}^f (nm)	h_w^g (nm)	$V_{me,open}^h$ (cm ³ /g)	$V_{me,blocked}^i$ (cm ³ /g)	V_{micro}^j (%)	$V_{me,open}^k$ (%)
SBA-15	59	353	9.70	0.70	660	0.16	0.54	7.00	2.70	0.54	0	23	100
PHTS-1	84	353	11.08	1.03	1040	0.29	0.74	6.79	4.30	0.23	0.51	28	31
PHTS-2	125	353	10.75	0.82	893	0.30	0.52	6.80	3.95	0.38	0.15	36	72
PHTS-3	146	353	9.29	0.44	580	0.17	0.27	5.68	3.62	<0.01	0.27	39	0
PHTS-4	125	373	9.52	0.66	779	0.25	0.41	7.00	2.52	0.08	0.33	38	19

^a Structural characteristics of four selected PHTS samples, synthesized as described in the experimental section, using indicated TEOS/P123 ratio and ageing temperature. ^b a_0 = lattice spacing. ^c V_{tot} = total pore volume (micropores and mesopores). ^d V_{mi} = micropore volume. ^e V_{me} = mesopore volume. ^f D_{pore} = pore diameter from the adsorption branch. ^g h_w = pore wall thickness. $h_w = a_0 - D_{pore}$. ^h $V_{me,open}$ = volume of open mesopores. ⁱ $V_{me,blocked}$ = volume of blocked mesopores. ^j V_{micro} (%) = percentage of micropores to total pore volume. ^k $V_{me,open}$ (%) - percentage of open mesopores to total mesopores.

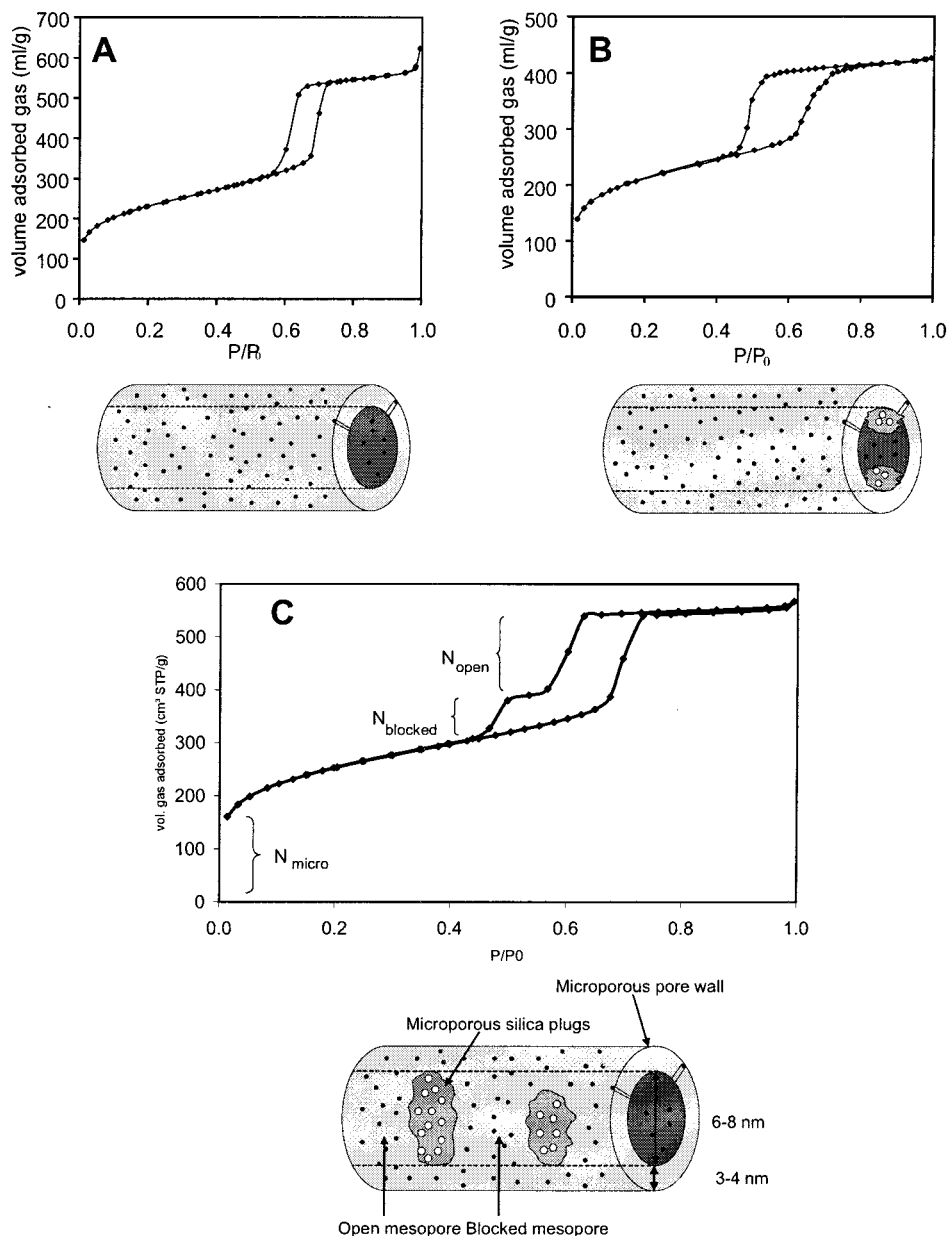


Figure 1. Nitrogen adsorption–desorption isotherms of (A) pore system with completely open mesopores and intrawall micropores (SBA-15); (B) pore system with blocked mesopore openings (ink-bottle pores) and intrawall micropores (PHTS-3), and (C) “plugged” mesopores, comprising both open and blocked mesopores, intrawall micropores, and microporous silica nanocapsules (PHTS-2).

The solution was stirred for 4–8 h at room temperature and then aged for 16 h at various temperatures. The white solid was filtered, washed, and calcined at 823 K.

X-ray diffractograms were recorded on a Philips PW1840 powder diffractometer, using Ni-filtered Cu K α radiation. Porosity and surface area studies were performed on a Quan-

tachrome Autosorb-1-MP automated gas adsorption system. The calcined samples were degassed for 17 h at 200 °C. Gas adsorption was measured using nitrogen as the adsorbate at liquid nitrogen temperature.

TEM pictures were recorded on a Philips CM200 microscope in bright field transmission mode.

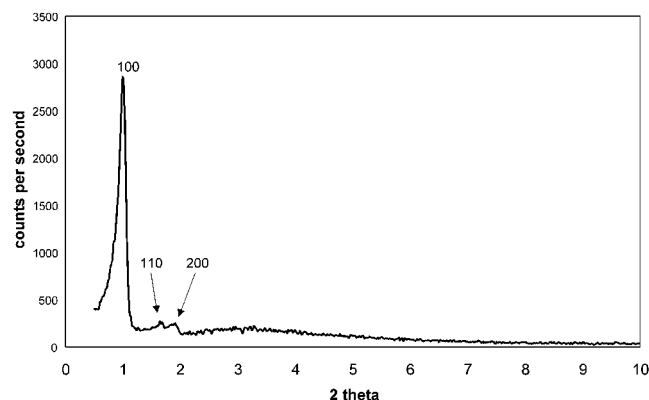


Figure 2. X-ray diffractogram of a PHTS material (PHTS-2).

Results and Discussion

We have prepared a broad range of materials with distinctly different characteristics by changing the synthesis parameters (surfactant/TEOS ratio, synthesis temperature, and time) in a controlled way. The synthesis conditions of a selected set of sample are shown in Table 1. The 77 K nitrogen adsorption–desorption isotherms of three distinctly different samples are shown in Figure 1.

All synthesized materials exhibit the typical X-ray diffraction patterns of the 2D hexagonal pore ordering in the $p6mm$ space group,⁸ as illustrated by the representative pattern in Figure 2.

The isotherm in Figure 1A is typical for the SBA-15 material,⁸ a two-dimensional $p6mm$ structure formed by open cylindrical mesopores greater than ca. 5 nm in diameter. The isotherm in Figure 1B shows the isotherm of a material with regular cylindrical mesopores that are accessible only through permeable microporous plugs. This is evident from the desorption branch of the isotherm and the shape of the hysteresis loop, characteristic of ink-bottle pores.¹⁶ The isotherm in Figure 1C is remarkable. It has the following characteristic features: (1) adsorption in intrawall micropores at low relative pressures; (2) multilayer adsorption in regular mesopores and capillary condensation in narrow intrawall mesopores; (3) a one-step capillary condensation, indicating uniform mesopores; (4) a two-step desorption branch indicating the pore blocking effects (sub-step at the relative pressure of ca. 0.45).

Combined with the typical $p6mm$ XRD pattern (Figure 2) for a hexagonally ordered structure, the adsorption–desorption behavior is consistent with the structure comprising open and closed cylindrical mesopores, as explained in Figure 3. Assuming a hemispherical shape of the plugs and using the Derjagium–Broekhoff–de Boer approximation (see ref 16 and references therein) for the attractive interactions with the pore walls, it can be shown that for a typical $R_{\text{cyl}} = 3.5$ nm pore, the equilibrium meniscus is not formed during the adsorption process if $R_{\text{plug}} > \text{ca. } 1.5 R_{\text{cyl}}$. In this case, the condensation pressure is determined by R_{cyl} . Thus, capillary condensation in both open and closed sections occurs at the same relative pressure, when the metastable adsorption film on the cylindrical surface loses its stability.¹⁷ In the open sections, the desorption occurs at equilibrium conditions via receding meniscus (the high-pressure desorption step). In the closed sections of the pore, the desorption is delayed until the vapor pressure is reduced below the limit of stability of condensed nitrogen, to ca. $p/p_0 = 0.45$. This pressure depends very weakly on the pore size and pore geometry.¹⁶

This interpretation is fully supported by the nonlocal density functional theory (NLDFT) and molecular simulations of

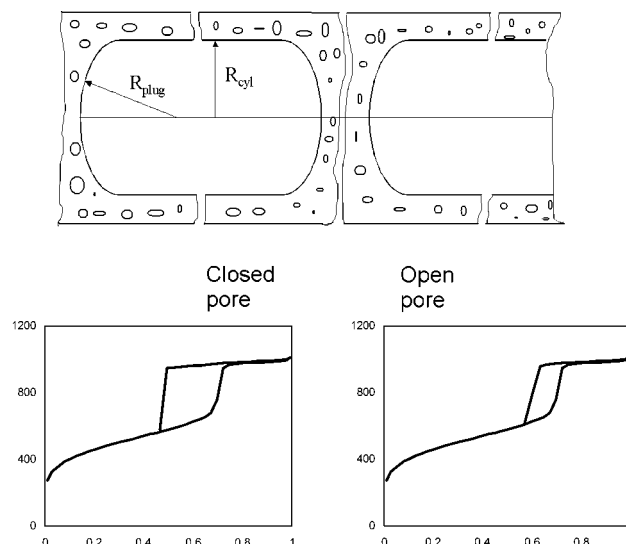


Figure 3. Schematic representation of the adsorption process in open and blocked (ink-bottle) cylindrical pores.

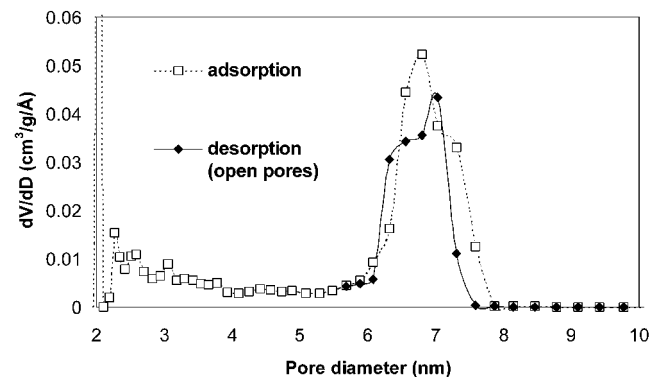


Figure 4. NLDFT pore size distribution of a PHTS material (PHTS-2).

adsorption and hysteresis in cylindrical pores.¹⁷ Particularly, the shape and width of the hysteresis loop between the capillary condensation and the high-pressure desorption steps agree quantitatively with the theoretical predictions for cylindrical pores.

The mesopore size distribution (Figure 4) and the total amount of micropores are calculated from the adsorption branch of the isotherm by the NLDFT method.^{17b} The fractions of open and closed mesopores have been determined from the pore size distributions. Materials exhibiting the isotherm 1C and the $p6mm$ XRD pattern will be referred to a PHTS (plugged hexagonal templated silica).

Using a Philips CM200 microscope, we have investigated extensively the PHTS and SBA-15 samples in bright field transmission mode. In Figure 5 we show representative images for these materials. Both micrographs provide side-on views of the ordered mesopore system. While the mesopores in SBA-15 run smoothly over several micrometers of length, the PHTS displays smaller domain sizes for the ordered mesopores. Moreover, the wall thickness varies more strongly for the latter material.

The rather thick walls (~ 4 nm) of the large cylindrical mesopores are perforated with micropores. Moreover, the cylindrical mesopores themselves are “plugged” with amorphous silica nanocapsules, which are also microporous. These nanocapsules are created by a large excess of the silica source (TEOS) that is used in the synthesis and by rapid hydrolysis of the silicon alkoxide at the very low pH used in the synthesis.

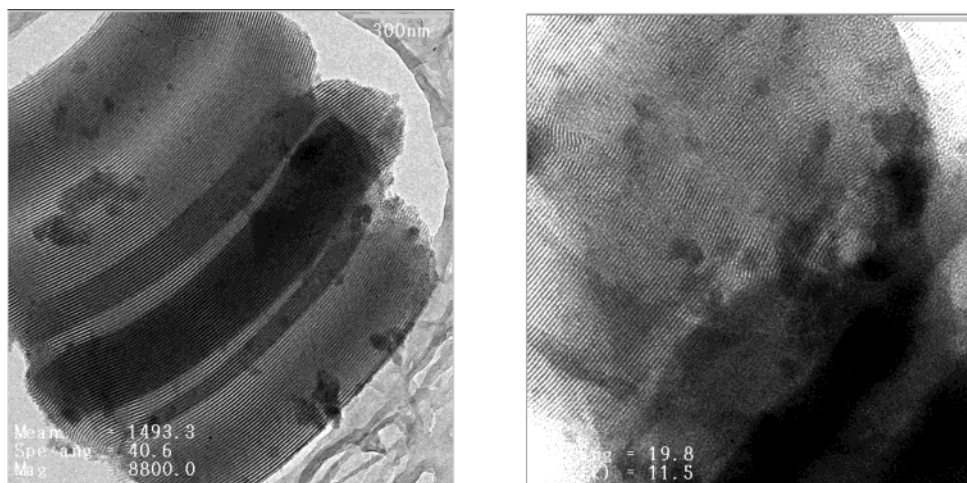


Figure 5. TEM pictures of SBA-15 (left) and PHTS-2 (right).

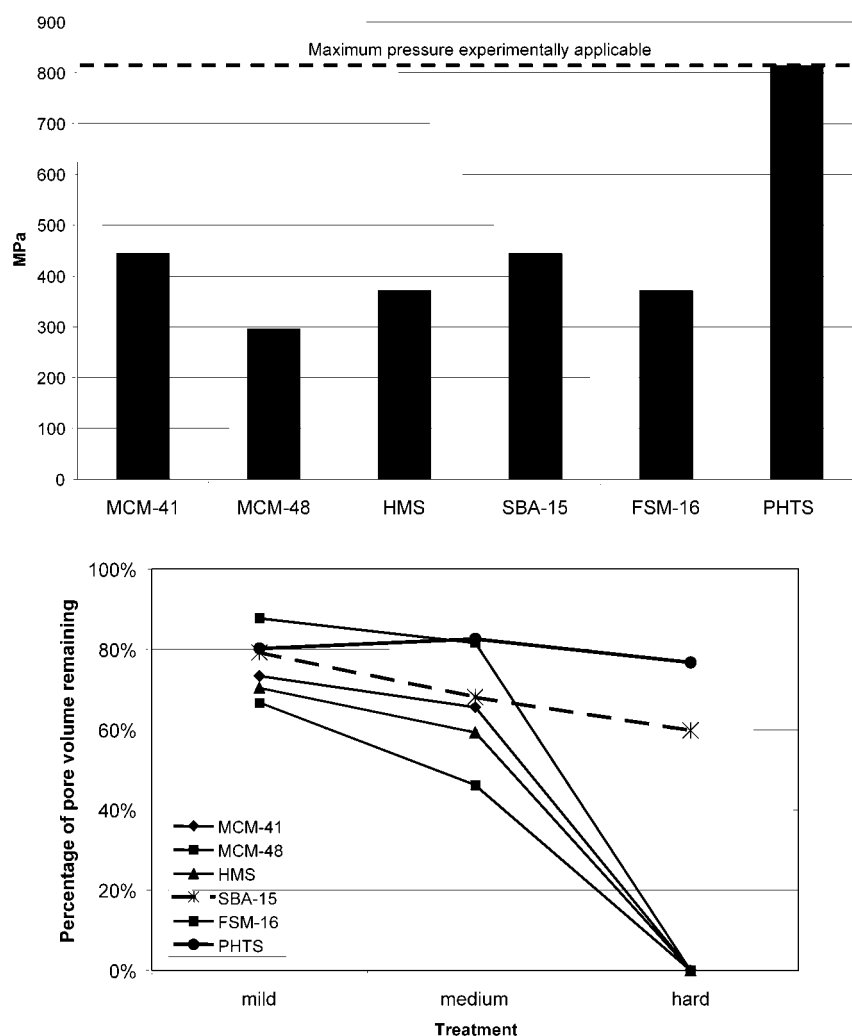


Figure 6. (A) Mechanical stability of the most common mesoporous templated materials. (B) Hydrothermal stability of the most common mesoporous templated materials. Description of treatments is as follows. Mild: nitrogen flow (25% water) at 1013 hPa and 673 K for 50 h. Medium: nitrogen flow (25% water) at 1013 hPa and 673 K for 120 h. Hard: steaming on a grid above the water in an autoclave at 393 K and autogenous pressure for 24 h.

The micropores in the silica walls can be explained by the penetration of hydrophilic poly(ethyleneoxide) chains of the triblock copolymer in the silica wall, as already suggested by Kruk et al.⁹ The microporosity of the plugs may have a different origin. It is known that Pluronic triblock copolymers are in fact polydisperse mixtures of several triblock copolymers with a wide range of molecular weights and that they contain appreciable

amounts of diblock copolymers and even free PO chains. Some of these components, especially the low molecular weight ones, may not be involved in the actual templating of the mesopores, but still act as templates for the disordered nanocapsules, inducing a complementary porosity. The mesopores themselves are created by the so-called charge compensating templating mechanism of the entire triblock copolymer.

Table 1 shows the synthesis conditions and the characteristics of a very limited number of synthesized samples. The thickness of the mesoporous walls is typically 3–4 nm, which is excellent, compared to a typical wall thickness of 1 nm for the well-known MCM-41 structure. Very high total pore volumes (up to 1 cm³/g) and micropore volumes (up to 0.3 cm³/g) can be obtained. Especially the contribution of micropores (with contributions of both micropores in the walls and micropores in the silica nanocapsules) has an unprecedented high value. Both the ratio micropore/mesopore volumes as the ratio of open/closed mesopores are tuneable in a wide range. Comparison of samples SBA-15 and PHTS-(1–3) shows the important effect of the surfactant/TEOS ratio on the sample characteristics. With increasing TEOS concentrations, the surface area and total pore volume gradually decrease, and the pore diameter decreases systematically. The amount of “open” mesopores is variable from 100% for a regular SBA-15 to 0% for PHTS-3. Although the pore volume decreases with increasing TEOS concentration, the relative contribution of micropores increases. This is another strong support for the statement that the silica nanocapsules are microporous by themselves. PHTS-4 is to be compared with PHTS-2 and shows the effect of an elevation of the aging temperature from 353 to 373 K. The average pore diameter is enlarged and the wall thickness decreases from 3.9 to 2.5 nm. These effects are also observable for regular SBA-15 and are explained by the increasing hydrophobicity of the ethyleneoxide chains at higher temperatures.⁹

The thermal, hydrothermal, and mechanical stability of the PHTS materials is excellent. Figure 6A shows the mechanical stability of the most common mesoporous templated materials.¹⁸ The maximum pressure that a material could withstand was defined as the pressure at which the material lost either more than 50% of its pore volume or 50% of the most intensive diffraction band after applying that pressure for 5 min. It is obvious from this graph that all conventional materials are relatively unstable toward unilateral pressure. The PHTS material on the other hand can withstand very high pressures. The maximum pressure indicated in the graph is the maximum pressure that could be achieved by our experimental setup. Figure 6B shows the hydrothermal stability of the same materials. Three different treatments were tested. The treatments, denoted “mild” and “medium” consist of flowing nitrogen, saturated with 25% water vapor through the sample bed at atmospheric pressure at 673 K for 50 and 120 h, respectively. The “hard” treatment consists of placing the sample on a grid just above an excess of liquid water in an autoclave and subsequently heating the autoclave at 393 K for 24 h at autogenous pressure. Despite the fact that most of these materials are synthesized with the same silica source (TEOS), SBA-15 and PHTS are hydrothermally much more stable than, for instance, HMS and MCM-41, which also have a hexagonal structure. It is reasonable to suggest that this higher hydrothermal

stability is a result of the thicker pore walls. This had already been suggested for SBA-15.¹⁹ It is believed that the structural degradation is caused by the hydrolysis of Si–O–Si bonds.²⁰ If the walls are thin, as in the case of HMS, FSM-16, MCM-41, and MCM-48 (thickness of ~10 Å, which is only a few [SiO₄]⁴⁻ groups), these structures collapse easily by hydrolysis.

Conclusions

In conclusion, a completely new type of porous templated material has been synthesized in a very simple and fast way. The material consists of mesoporous cylinders, consisting of microporous walls. Moreover, microporous silica nanocapsules are present inside the cylindrical mesopores. The structure is fully confirmed by nitrogen adsorption and the NLDFT theory, TEM, and XRD. The micropore volume of these structures and their stability are unprecedented.

Acknowledgment. This research was funded by a grant from the University of Antwerp (Special Research Fund) and by the F.W.O. (Flemish Fund for Scientific Research). The authors are grateful to Mrs. Sandra Kemp for making the 2D-TEM images. P.V.D.V. acknowledges the FWO-Flanders for financial support.

References and Notes

- (1) Kresge, C. T.; Leonowicz, M. E.; Roth, W. J.; Vartuli, J. C.; Beck, J. S. *Nature* **1992**, 359, 710.
- (2) Inagaki, S.; Fukushima, Y.; Kuroda, K. *Chem. Commun.* **1993**, 680.
- (3) Yanagisawa, T.; Shimizu, T.; Kuroda, K.; Kato, C. *Bull. Chem. Soc. Jpn.* **1990**, 63, 988.
- (4) Tanev, P. T.; Pinnavaia, T. J. *Science* **1995**, 267, 865.
- (5) Tanev, P. T.; Chibwe, M.; Pinnavaia, T. J. *Nature* **1994**, 368, 321.
- (6) Bagshaw, S. A.; Prouzet, E.; Pinnavaia, T. J. *Science* **1995**, 269, 1242.
- (7) Zhao, D.; Feng, J.; Huo, Q.; Melosh, N.; Fredrickson, G. H.; Chmelka, B.; Stucky, G. D. *Science* **1998**, 279, 548.
- (8) Zhao, D.; Huo, Q.; Feng, J.; Chmelka, B.; Stucky, G. D. *J. Am. Chem. Soc.* **1998**, 120, 6024.
- (9) Kruk, M.; Jaroniec, M.; Ko, C. H.; Ryoo, R. *Chem. Mater.* **2000**, 12, 1961.
- (10) Miyazawa, K.; Inagaki, S. *Chem. Commun.* **2000**, 2121.
- (11) Sakamoto, Y.; Kaneda, M.; Terasaki, O.; Zhao, D. Y.; Kim, J. M.; Stucky, G. D.; Shin, H. Y.; Ryoo, R. *Nature* **2000**, 408, 449.
- (12) Weckhuysen, B. M.; Rao, R. R.; Pelgrims, J.; Schoonheydt, R. A.; Bodart, P.; Debras, G.; Collart, O.; Van Der Voort, P.; Vansant, E. F. *Chem. Eur. J.* **2000**, 6, 2960.
- (13) Clark, J. H. *Green Chem.* **1999**, 1, 1.
- (14) Corma, A. *Chem. Rev.* **1997**, 97, 2373.
- (15) Karlsson, A.; Stöcker, M.; Schmidt, R. *Microporous Mesoporous Mater.* **1999**, 27, 181.
- (16) Ravikovitch, P. I.; Neimark, A. V. *Langmuir* **2002**, 18, 1550.
- (17) (a) Neimark, A. V.; Ravikovitch, P. I.; Vishnyakov, A. *Phys. Rev. E* **2000**, 62, R1493. (b) Ravikovitch, P. I.; Neimark, A. V. *J. Phys. Chem. B* **2001**, 105, 6817.
- (18) Cassiers, K.; Linssen, T.; Mathieu, M.; Benjelloun, M.; Schrijnemakers, K.; Van Der Voort, P.; Cool, P.; Vansant, E. F. *Chem. Mater.* **2002**, in press.
- (19) Mokaya, R. *J. Phys. Chem. B* **1999**, 103, 10204.
- (20) Tatsumi, T.; Koyano, K. A.; Tanaka, Y.; Nakata, S. *Chem. Lett* **1997**, 5, 469.